DOI: 10.1002/chem.200601312

Interplay Between Kinetically Slow Thermal Spin-Crossover and Metastable High-Spin State Relaxation in an Iron(II) Complex with Similar $T_{1/2}$ and T(LIESST)

Victoria A. Money,[a] Chiara Carbonera,[b] Jérôme Elhaïk,[c] Malcolm A. Halcrow,*[c] Judith A. K. Howard,*[a] and Jean-François Létard*[b]

Abstract: This paper describes the first material to show the well-known light-induced excited spin-state trapping (LIESST) effect, the metastable excited state of which relaxes at a temperature approaching its thermal spin-crossover. Cooling polycrystalline $[FeL_2][BF_4]_2 \cdot x H_2O$ (L = 2,6-bis{3-methylpyrazol-1-yl}pyridine; $x = 0$–$^1/_3$) at 1 K min^{-1} leads to a cooperative spin transition, taking place in two steps centered at 147 and 105 K, that is only 54% complete by magnetic susceptibility. Annealing the sample at 100 K for 2 h results in a slow decrease in $\chi_M T$ to zero, showing that the remainder of the spin-crossover can proceed, but is kinetically slow. The crystalline high- and fully low-spin phases of $[FeL_2][BF_4]_2 \cdot x H_2O$ are isostructural ($C2/c$, $Z = 8$), but the spin-crossover proceeds via a mixed-spin intermediate phase that has a triple unit cell ($C2/c$, $Z = 24$). The water content of the crystals is slowly lost on exposure to air without causing decomposition. However, the high-spin/mixed-spin transition in the crystal proceeds at 110 ± 20 K when $x = {}^1/_3$ and 155 ± 5 K when $x = 0$, which correspond to the two spin-crossover steps seen in the bulk material. The high-spin state of the compound is generated quantitatively by irradiation of the low-spin or the mixed-spin phase at 10 K, and in approximately 70% yield by rapidly quenching the sample to 10 K. This metastable high-spin state relaxes back to the low-spin ground state at 87 ± 1 K in one, not two, steps, and without passing through the intermediate phase. This implies that thermal spin-crossover and thermally activated high-spin–low-spin relaxation in this material become decoupled, thus avoiding the physical impossibility of T-(LIESST) being greater than $T_{1/2}$.

Keywords: coordination chemistry · iron · magnetic properties · photomagnetism · spin crossover

Introduction

Spin-crossover transition-metal systems are some of the most intensively studied switchable molecular compounds.[1] Materials of this sort can interconvert between high-spin (HS) and low-spin (LS) electronic states in response to an external stimulus, which might be a change in temperature or pressure, or exposure of the sample to laser irradiation or a strong magnetic field. When cooperativity between spin centers in the sample is strong, a thermal spin transition may exhibit a thermal hysteresis loop of up to 60 K in width.[2] In this case a material is truly bistable within this hysteresis loop, since it can exist in either its HS or LS form in this temperature range depending on its history.[3] Moreover, by inducing a transition at low temperature it is often possible to trap a solid material in a metastable (usually HS) state; this is most commonly accomplished by laser irradiation at 10 K or below (termed light-induced excited spin-state trapping or LIESST effect).[4] This is particularly common in iron(II) spin-transition complexes, which have large structural differences between their HS and LS states.[5] This gives rise to increased quantum mechanical

[a] Dr. V. A. Money, Prof. J. A. K. Howard
Department of Chemistry, University of Durham
South Road, Durham DH1 3 LE (UK)
Fax: (+44) 191-384-4737
E-mail: j.a.k.howard@durham.ac.uk

[b] Dr. C. Carbonera, Dr. J.-F. Létard
Institut de Chimie de la Matière Condensée de Bordeaux
UPR CNRS No. 9048 - Université Bordeaux I
Groupe des Sciences Moléculaires
87 Av. Doc. A. Schweitzer, 33608 Pessac (France)
Fax: (+33) 540-002-678
E-mail: letard@icmcb-bordeaux.cnrs.fr

[c] Dr. J. Elhaïk, Dr. M. A. Halcrow
School of Chemistry, University of Leeds
Leeds LS2 9 JT (UK)
Fax: (+44) 113-343-6565
E-mail: M.A.Halcrow@leeds.ac.uk

Supporting information for this article is available on the WWW under http://www.chemeurj.org or from the author. It contains an additional figure showing the irreproducible susceptibility behavior shown by early samples of the material, the quantification of the water content of $[FeL_2][BF_4]_2 \cdot x H_2O$ by ^{1}H NMR, powder diffraction data and an overlay of the molecular structures of HS $[FeL_2][BF_4]_2 \cdot x H_2O$ at 200 and 30 K; and, all crystallographic data in CIF format.

tunneling barriers, which can prevent a metastable HS compound from relaxing back to its ground state until an activation temperature for thermal relaxation is reached.[6] In particularly favorable cases, the metastable spin state of the sample may be stable to thermally activated decay at temperatures up to 120 K,[7] although relaxation temperatures below 50 K are a lot more common in practice. This corresponds to another type of bistability, between the ground state and a kinetically trapped, metastable excited state of the same material, which can be interconverted photochemically below the relaxation temperature.

Since LS and HS forms of the same compound are often different colors, as well as having different magnetic moments, both types of bistability lend themselves to a variety of potential applications. For example, the use of spin-crossover (SCO) materials as components in optical displays[8,9] and dielectric memory devices,[10,11] and as MRI contrast agents[12] have all been demonstrated and, in some cases, patented.[8b,c,11] Spin-crossover effects are also important in some biological and geological systems.[13] For these reasons, the synthesis of new SCO materials, and the structural and physical chemistry underlying spin transitions and spin-trapping phenomena, are of very strong continuing interest.[1,9]

Since the stability of a LIESST excited state depends on the method used to measure it, we introduced the idea of quantifying this photomagnetic phenomenon by systematically determining the T(LIESST) values[14] of a range of materials using a standardized procedure.[15] Here, T(LIESST) represents the limiting temperature above which any light-induced HS information is erased inside the cavity of a SQUID magnetometer when the temperature is increased at the rate of 0.3 K min^{-1}. Through these experiments we have produced a database of more than sixty iron(II) spin-crossover materials with nitrogen-donor ligands,[15] and we have found that a simple linear relation governs the photomagnetic properties of most of these compounds [Eq. (1), Figure 1], in which $T_{1/2}$ is the thermal spin transition temperature and T_0 is an empirical parameter corresponding simply to the y intercept of the line defined by the data.[15]

$$T(\text{LIESST}) = T_0 - 0.3\,T_{1/2} \quad (1)$$

While the detailed physical origin of T_0 is uncertain, it appears to depend primarily on the geometry and conformational rigidity of the ligand donors about the metal ion. Factors outside the inner metal coordination sphere, such as intermolecular cooperativity, crystal packing, and the identity of any anions and solvent in the material, result in only minor perturbations to T_0 for a given set of metal complexes.[16] To date, four series of compounds showing parallel T_0 lines have been demonstrated, with values of 100 K (complexes of monodentate ligands),[17] 120 K (bidentate ligands),[17] 150 K (meridional tridentate ligands)[18–20] and 200 K (three-dimensional network solids).[21] Although it is purely an empirical relationship, Equation (1) has clear predictive value, and a current challenge is to design new materials with increased T_0 values to yield bistable materials the excited spin states of which can be trapped near room temperature. Since T(LIESST) and $T_{1/2}$ are inversely dependent on each other, from the inverse energy gap law,[22] there is a theoretical maximum possible value of T(LIESST) for each T_0 line, for which T(LIESST) and $T_{1/2}$ are equal (Figure 1). The rationale for this study was to investigate this limitation, by preparing a material whose thermal and photomagnetic properties exhibit this condition. No such compounds have been made before.

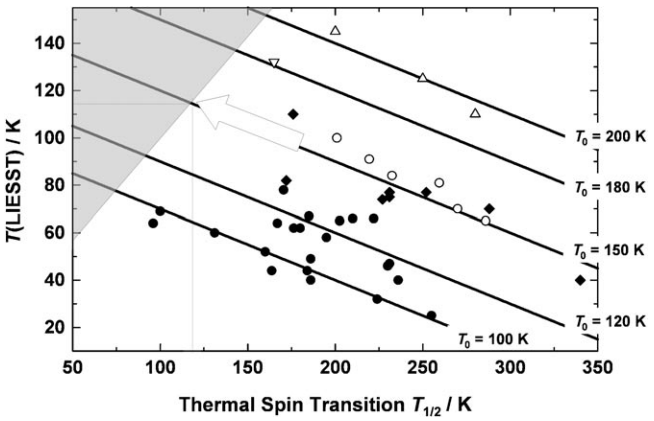

Figure 1. The relationship between the thermal- and light-induced spin transitions of the series of complexes based on the 2,6-dipyrazol-1-yl pyridine ligand, following the $T_0 = 150$ K line. The shaded area is where $T_{1/2}$ is predicted to be greater than T(LIESST).

For the past five years, we have been studying iron(II) complexes of tridentate 2,6-di(pyrazol-1-yl)pyridine and 2,6-di(pyrazol-1-yl)pyrazine ligands.[23] Different homoleptic complex salts of this series of ligands exhibit a variety of thermal spin-crossover regimes,[24–30] several of which are mediated by unusual structural chemistry.[28,29] Many of these transitions occur close to room temperature,[20,24,25,30] and the spin states of individual members of this series can be predicted qualitatively by considering the steric and inductive properties of any substituents on the ligand periphery.[31] Moreover, most of these compounds exhibit the LIESST phenomenon,[19,20,29] quantitatively forming long-lived trapped HS states, three of which we have been able to characterize crystallographically.[20,26,30] The thermal stability of these trapped HS states closely follows the $T_0 =$ 150 K line defined by Equation (1) that we had previously proposed for iron(II) complexes of tridentate nitrogen-donor ligands (Figure 1).[19,20] For these reasons, we decided to pursue iron complexes of 2,6-bis(3-methylpyrazol-1-yl)-pyridine (L).[32] Precedent suggests that the steric influence of the methyl substitutents in $[FeL_2]^{2+}$, which lie close to the inner coordination sphere about the metal ion, should stabilize its HS state to a small extent, thus lowering its thermal spin-transition value.[31,33] This paper describes the fascinatingly complex spin-crossover

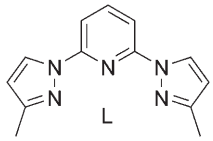

behavior exhibited by $[FeL_2][BF_4]_2{\cdot}x\,H_2O$ ($x=0$–$^1/_3$), whose thermal spin transition does indeed occur at a point on the $T_0=150$ K line at which T(LIESST) and $T_{1/2}$ are predicted to be very close (Figure 1). Surprisingly, and uniquely, the proximity of these transition temperatures is avoided by the thermal spin-crossover and LIESST relaxation processes in this material becoming separated from one other.

Experimental Section

The complex $[FeL_2][BF_4]_2$ was prepared as described previously.[32] Diffusion of diethyl ether vapor into a solution of the crude material in methanol yielded yellow prisms of formula $[FeL_2][BF_4]_2{\cdot}x\,H_2O$.

Crystallography: Crystallographic data were collected on a Bruker APEX diffractometer equipped with a molybdenum microsource[34] (ω-scan, 0.3°/frame) with graphite-monochromated $Mo_{K\alpha}$ radiation ($\lambda=$ 0.71073 Å). Between 360 and 110 K the crystals were cooled in a flow of chilled nitrogen gas by using an Oxford Cryosystems Cryostream.[35] Below 110 K cooling was carried out in a flow of chilled helium with an Oxford Cryosystems HELIX.[36,37] All data processing was carried out by using the SAINT[38] and XPREP[39] software packages. Absorption corrections were applied using SADABS.[39] The structures were solved by direct methods and refined on F^2 using full matrix least-squares methods within the SHELXTL suite.[39] The hydrogen atoms were placed geometrically and treated with a riding model. For the LIESST experiments the samples were irradiated for ten minutes with a He:Ne laser ($\lambda=$ 632.8 nm, 25 mW), whilst on the diffractometer. Selected crystallographic parameters are presented in Tables 1–3.

CCDC-631048–631057 contain the supplementary crystallographic data for this paper. These data can be obtained free of charge from The Cambridge Crystallographic Data Centre via www.ccdc.cam.ac.uk/data_request/cif.

Table 1. Selected crystallographic parameters for $[FeL_2][BF_4]_2$ at 200, 130, and 90 K.

formula	$C_{26}H_{26}B_2F_8FeN_{10}$	$C_{26}H_{26}B_2F_8FeN_{10}$	$C_{26}H_{26}B_2F_8FeN_{10}$
M_r	708.04	708.04	708.04
spin state	high spin	mixed spin	low spin
T [K]	200	130	90
shape	irregular	irregular	irregular
color	yellow	yellow	brown
crystal system	monoclinic	monoclinic	monoclinic
space group	$C2/c$	$C2/c$	$C2/c$
a [Å]	23.341(5)	54.88(1)	22.707(5)
b [Å]	11.000(2)	10.892(2)	10.817(2)
c [Å]	24.037(5)	31.997(6)	24.162(5)
β [°]	95.44(3)	109.77(3)	93.11(3)
V [Å^3]	6144(2)	17999(6)	5926(2)
Z	8	24	8
ρ_{calcd} [Mg m^{-3}]	1.531	1.568	1.587
μ [mm^{-1}]	0.576	0.590	0.598
crystal size [mm]	0.20×0.16×0.12	0.20×0.16×0.12	0.20×0.16×0.12
θ range [°]	1.70 to 23.26	1.32 to 35.00	1.69 to 35.02
reflns collected	8676	49319	14609
independent reflns	4105	28791	9088
$R_{(int)}$	0.0382	0.0583	0.0712
$wR(F^2)$ (all data)	0.1437	0.2331	0.2944
$R(F)$ (all data)	0.0510	0.1361	0.1421
parameters	428	1282	428
GOF	1.132	1.017	1.027
max/min $\Delta\rho$ [e Å^{-3}]	0.47/−0.49	2.09/−1.34	2.04/−2.32

Table 2. Selected crystallographic parameters for $[FeL_2][BF_4]_2{\cdot}^1/_3H_2O$ at 200 K, 130 K and 90 K.

formula	$C_{26}H_{26}B_2F_8FeN_{10}$	$C_{26}H_{26}B_2F_8FeN_{10}$	$C_{26}H_{26}B_2F_8FeN_{10}$
M_r	708.04	708.04	708.04
spin state	high spin	high spin	mixed spin
T [K]	200	130	90
shape	prism	prism	prism
color	yellow	yellow	brown
crystal system	monoclinic	monoclinic	monoclinic
space group	$C2/c$	$C2/c$	$C2/c$
a [Å]	23.425(5)	23.285(5)	55.28(1)
b [Å]	11.000(2)	10.965(2)	10.957(2)
c [Å]	24.017(5)	23.914(5)	31.973(6)
β [°]	95.56(3)	95.63(3)	108.88(3)
V [Å^3]	6159(2)	6076(2)	18325(6)
Z	8	8	24
ρ_{calcd} [Mg m^{-3}]	1.540	1.560	1.551
μ [mm^{-1}]	0.577	0.584	0.581
crystal size [mm]	0.16×0.13×0.11	0.16×0.13×0.11	0.16×0.13×0.11
θ range [°]	1.70 to 26.33	1.71 to 26.05	0.78 to 26.06
reflns collected	16308	15666	41067
independent reflns	5371	5220	15090
$R_{(int)}$	0.0219	0.0230	0.1135
$wR(F^2)$ (all data)	0.1462	0.1537	0.4464
$R(F)$ (all data)	0.0606	0.0630	0.2352
parameters	432	432	585
GOF	1.120	1.139	1.285
max/min $\Delta\rho$ [e Å^{-3}]	0.87/−0.38	1.02/−0.45	3.86/−1.46

Reflectivity measurements: The reflectivity was investigated by using a home-built reflectivity setup coupled with a CVI spectrometer; this setup allowed us both to collect the reflectivity spectra in the 450–950 nm range at a given temperature, and to follow the temperature dependence of the signal at a selected wavelength (±2.5 nm) between 5 K and 290 K. The instrument was also equipped with an optical detector, which collected the whole reflected intensity and gave the total reflectivity signal as a function of temperature. The source of white light consisted of a halogen lamp emitting between 300 and 2400 nm. This analysis was performed directly on a thin layer of the available solid samples in the form of a polycrystalline powder without any dispersion in a matrix. It was checked that no change in the powder was recorded after a thermal cycle.

Magnetometry: Magnetic measurements were performed on polycrystalline powder samples weighing 19.6 mg by using a MPMS-55 Quantum Design SQUID (Superconducting Quantum Interference Device) magnetometer operating $H=2$ T between 2–300 K at atmospheric pressure, with a speed of 10 K min^{-1} in the settle mode, giving an effective temperature ramp of 0.3 K min^{-1}. The data were corrected for the magnetization of the sample holder and for diamagnetic contributions from Pascal's constants.[40]

The photomagnetic measurements were performed by using a Spectrum Physics Series 2025 Kr^+ laser ($\lambda=532$ nm) coupled by means of an optical fiber to the cavity of an MPMS-55 Quantum Design SQUID magnetometer and the power at the sample surface was adjusted to 5 mW cm^{-2}. It was noted that there was no change in the data due to heating of the sample. For the photomagnetic experiments the samples consisted of a thin layer of compound, the weight of which was obtained by comparison of the thermal spin-crossover curve with that of a more accurately weighed sample of the same compound. Our previously published, standardized method for determining LIESST properties was followed.[14] After cooling slowly to 10 K the sample, now in the LS state, was irradiated, and the change in magnetism followed. When the saturation point had been reached the light was switched off and the temperature increased at a rate of 0.3 K min^{-1} with the magnetization measured every 1 K. T(LIESST) was determined from the minimum of the $\partial\chi_M T/\partial T$ versus T curve for the relaxation process.

Table 3. Selected crystallographic parameters for $[FeL_2][BF_4]_2 \cdot {}^1/_3\,H_2O$ after flash freezing to 30 K, after cooling from 300 K at 120 K h^{-1}, after irradiation of the slow cooled crystal and after cooling from 100 to 30 K.

	Flash freezing	Cool at 120 K/hr	After irradiation	Cooling from 100 K
formula	$C_{26}H_{26}B_2F_8FeN_{10}O_{0.33}$	$C_{26}H_{26}B_2F_8FeN_{10}O_{0.33}$	$C_{26}H_{26}B_2F_8FeN_{10}O_{0.33}$	$C_{26}H_{26}B_2F_8FeN_{10}O_{0.33}$
M_r	713.38	713.38	713.38	713.38
spin state	high spin	mixed spin	high spin	low spin
T [K]	30	30	30	30
shape	irregular	irregular	irregular	prism
color	yellow	brown	yellow	brown
crystal system	monoclinic	monoclinic	monoclinic	monoclinic
space group	$C2/c$	$C2/c$	$C2/c$	$C2/c$
a [Å]	23.229(5)	54.91(1)	23.078(5)	22.789(5)
b [Å]	10.935(2)	10.872(2)	10.948(2)	10.836(2)
c [Å]	23.801(5)	31.710(6)	23.797(5)	24.023(5)
β [°]	96.02(3)	108.94(3)	95.66(3)	93.86(3)
V [Å^3]	6012(2)	17905(6)	5983(2)	5919(2)
Z	8	24	8	8
ρ_{calcd} [Mg m^{-3}]	1.576	1.588	1.584	1.601
μ [mm^{-1}]	0.590	0.595	0.593	0.600
crystal size [mm]	$0.25\times0.24\times0.12$	$0.25\times0.24\times0.12$	$0.25\times0.24\times0.12$	$0.25\times0.20\times0.15$
θ range [°]	1.76 to 28.31	0.78 to 28.30	2.63 to 28.02	0.170 to 28.40
reflns collected	22123	42076	16766	15639
independent reflns	6696	18466	5856	6466
$R_{(int)}$	0.0372	0.0790	0.0190	0.0311
$wR(F^2)$ (all data)	0.1486	0.3255	0.0965	0.4885
$R(F)$ (all data)	0.0742	0.1802	0.0433	0.2035
parameters	432	585	432	197
GOF	1.041	1.039	1.072	2.060
max/min $\Delta\rho$ [e Å^{-3}]	1.62/−0.57	3.56/−1.38	0.59/−0.33	4.98/−1.86

Other measurements: Powder diffraction data were obtained with a PANalytical X'Pert MPD diffractometer with Cu radiation (λ = 1.5418 Å). ^{1}H NMR spectra were run using a Bruker ARX250 spectrometer operating at 250.1 MHz. IR spectra were run as nujol mulls pressed between NaCl plates using a Nicolet Avatar 360 spectrophotometer.

Results and Discussion

Synthesis and magnetochemistry of $[FeL_2][BF_4]_2 \cdot x\,H_2O$: As we have reported previously, crystallization of $[FeL_2][BF_4]_2$ from MeCN/Et_2O affords a solvate $[FeL_2][BF_4]_2 \cdot 4\,MeCN$ that undergoes a complete, but very gradual, thermal spin transition centered near 175 K from a variable-temperature crystallographic study.[32] However, the variable-temperature susceptibility behavior of dried, bulk samples of $[FeL_2][BF_4]_2$, crystallized from MeCN, acetone or $MeNO_2$, was unusual and very sample-dependent (see Supporting Information). Visual inspection and unit cell determinations on single crystalline samples grown from these solvents established that the complex crystallizes as mixtures of phases, which always included a hydrate of formula $[FeL_2][BF_4]_2 \cdot x\,H_2O$. This phase can be prepared in pure form by recrystallization from MeOH/Et_2O, and all the experiments described below used material obtained in this way. The water content "x" varies between 0–$^1/_3$ by crystallography, depending on the age of the sample. Unfortunately this is too small to detect reliably by microanalysis, while the characteristic broad H-O-H bending vibration at 1630 cm^{-1} in the IR spectrum of the lattice hydrates[41] was obscured by two strong vibrations from the "L" ligand, at 1593 and 1626 cm^{-1}. However, the paramagnetic ^{1}H NMR spectrum of freshly crystallized $[FeL_2][BF_4]_2 \cdot x\,H_2O$ in pre-dried CD_3NO_2 did show a water peak at 2.3 ppm, that integrated to 0.6 ± 0.1 H relative to the other peaks from the L ligand (that is, $x = 0.3$). The phase purity of our $[FeL_2][BF_4]_2 \cdot x\,H_2O$ was confirmed by powder diffraction data at 200 K, which showed excellent agreement with that predicted from its crystal structure at that temperature (see Supporting Information).

However, even phase-pure $[FeL_2][BF_4]_2 \cdot x\,H_2O$ showed sample-dependent magnetic behavior. Fresh powder samples showed a pronounced plateau in their spin transition, which occurred in two steps centered near 110 and 140 K. In older samples, which had been stored for three months, this plateau was much narrower or missing altogether, with the entire spin transition taking place around 140 K (see Supporting Information). The origin of the plateau relates to the water content of the sample, which is slowly lost upon exposure to air; this is described in more detail below. All the magnetic and photomagnetic experiments described below were carried out using the same polycrystalline sample, which was approximately three weeks old.

Figure 2 shows the thermal spin transition measured from this sample in both the cooling and warming mode at a rate of 1 K min^{-1}. The complex is completely HS at 300 K, showing $\chi_M T = 3.5$ cm^3 K mol^{-1}.[40] On cooling the compound undergoes a partial spin transition between 150 and 90 K, occurring in two steps that both show a pronounced hysteresis. The first of these steps is centered at 147 K, with a hysteresis width of 6 K, while the second step is centered at 105 K

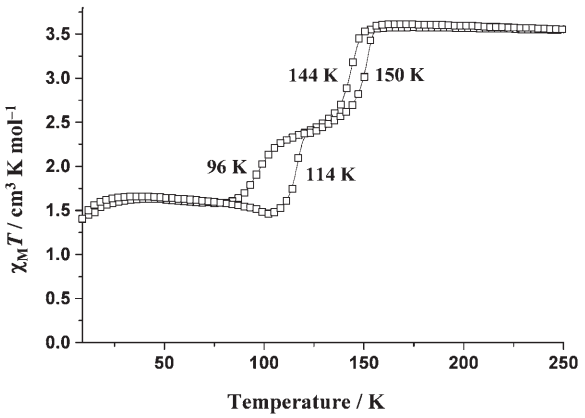

Figure 2. The thermal spin transition in warming and cooling modes of $[FeL_2][BF_4]_2{\cdot}x\,H_2O$, at a scan rate of 1 K min^{-1}.

with an 18 K hysteresis loop. The spin transition is incomplete, with a final $\chi_M T$ value of 1.6 cm^3 K mol^{-1} rather than the 0 cm^3 K mol^{-1} expected for a complete LS iron(II) species. This suggests that approximately 46% of the material remains in its HS state after cooling.

Equation (1) with $T_0 = 150$ K implies that any LIESST excited state associated with the partial spin transition at $T_{1/2} = 105$ K should decay at 118 K. It is physically impossible for T(LIESST) to be greater than $T_{1/2}$ in practice, but the similar values of these parameters imply that kinetic effects could play a substantial role in spin-crossover in this compound. To investigate this further, the experiment shown in Figure 3 was carried out. The sample was first cooled from room temperature to 100 K then poised at that temperature, and the evolution of the susceptibility measured over a two hour period (Figure 3a, stage 1). A dramatic decrease of the magnetic signal was observed during that time, reaching a final $\chi_M T \approx 0$ cm^3 K mol^{-1}, as expected for a completely LS iron(II) species. The sample was then cooled to 10 K (Figure 3b, stage 2), with $\chi_M T$ remaining close to 0 cm^3 K mol^{-1}. On warming from 10 K the sample remains fully LS until 115 K (stage 3) when then there is a sudden increase in $\chi_M T$ to 2.5 cm^3 K mol^{-1} (stage 4) followed by a short plateau (stage 5) and another abrupt increase (stage 6) to reach the fully HS state at 160 K with $\chi_M T = 3.5$ cm^3 K mol^{-1} (stage 7). The sample was then cooled again from this temperature (stages 8–12), and was found to undergo an incomplete thermal spin transition identical to that observed initially before cycling through the low-spin state (Figure 2).

Figure 4 shows the evolution of the susceptibility measured over a two hour period at 150, 140, 130, 120 and 100 K, respectively. In each case, the stationary limit

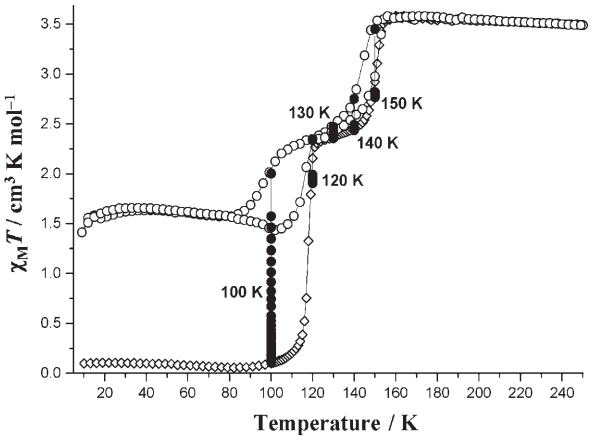

Figure 4. Kinetic studies of spin-crossover in $[FeL_2][BF_4]_2{\cdot}x\,H_2O$. The black circles show the change in susceptibility of the sample over a two hour period at 100, 120, 130, 140, and 150 K. For comparison, the original data from Figure 2 are also shown as open circles and diamonds.

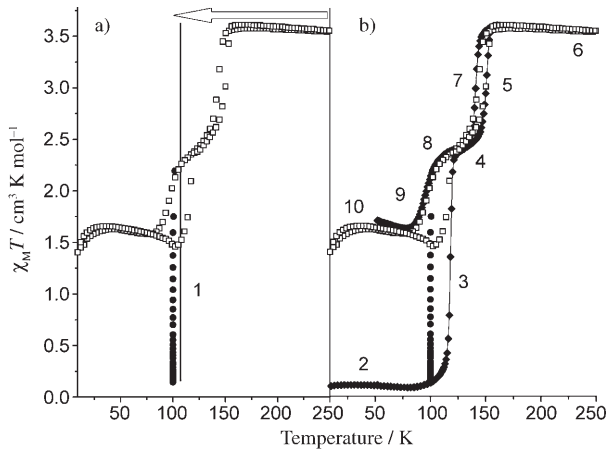

Figure 3. The thermal spin transition and relaxation of $[FeL_2][BF_4]_2{\cdot}x\,H_2O$. a) The sample is rapidly cooled to 100 K, and annealed at that temperature for 2 h. The black circles show the change in susceptibility of the sample during that period. b) The temperature of the resultant low-spin material is scanned at 1 K min^{-1}, through the ranges 100→5→250→50 K (see text for more details). For comparison, the original data from Figure 2 are also shown as open squares.

reached by the magnetic signal corresponds to the thermal spin-crossover behavior recorded from an almost quantitative LS state on the warming curve (see the experiment carried out in Figure 3). Clearly the shape of the thermal spin-crossover transition between 100–120 K is strongly dependent on the conditions used for cooling the sample, while above 130 K kinetic effects are negligible. Hence, the plateau in the susceptibility curve between 115 and 145 K is genuine.

Photomagnetism and excited spin-state trapping: The photomagnetic properties of $[FeL_2][BF_4]_2{\cdot}x\,H_2O$ were first screened by using variable-temperature reflectance visible spectroscopy. Figure 5 shows the modification of the absorption spectra of the complex recorded as function of the temperature and light irradiation, while the inset graph follows the temperature dependence of the reflectance intensity at 650 ± 2.5 nm. At room temperature, the visible spectrum is essentially constituted by a broad band at 850 nm, assignable to the d–d transition of the HS state, while on cooling to 150 K a new band is formed near 650 nm which corresponds

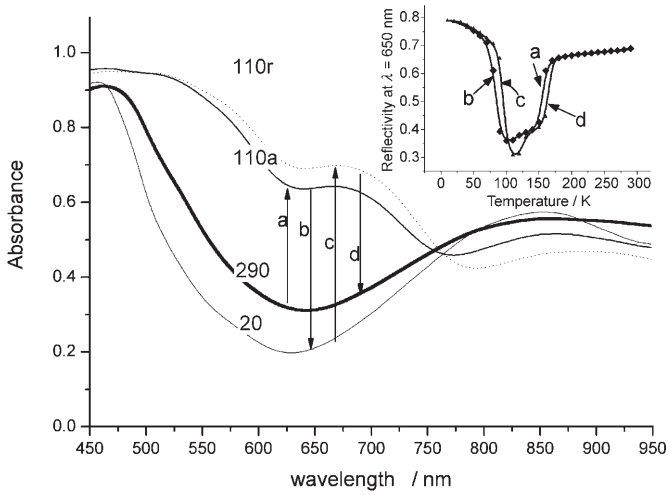

Figure 5. Changes in the reflectivity spectra of $[FeL_2][BF_4]_2$ upon warming and cooling. The inset shows the intensity of the absorption at 650 nm under the same conditions.

to the d–d and/or MLCT transitions of a LS fraction of the material (arrow a in Figure 5). Interestingly, these changes are reversed upon further cooling below 100 K, so that the fully HS spectrum is essentially reformed at 20 K (arrow b). This behavior is reversible upon re-warming (arrows c and d). These results are consistent with the occurrence of a thermal spin transition at around 150 K, and with the population at low temperatures of a light-induced metastable state that is induced by the light source used for recording the reflectivity spectra. Comparison of the cooling and arming cycles of the experiment (Figure 5 inset) shows small hysteresis loops at around 150 and 90 K. The former reflects the hysteresis in the thermal spin-conversion undergone by the material (Figure 1), while that at 90 K is a manifestation of the known light-induced thermal hysteresis (LITH) phenomenon.[42] The observation of a LITH effect implies a degree of intermolecular cooperativity in the relaxation of the photoinduced HS state in this compound.

Figure 6 shows the result of the photomagnetic experiments recorded by using a SQUID magnetometer. Before irradiation, the sample was precooled to 100 K and maintained at this temperature for 3 h, to generate the fully LS form of the material. Then at 10 K, the LS sample was irradiated with green laser light ($\lambda = 532.06$ nm). There was an abrupt increase in magnetic susceptibility that reached saturation at a value for $\chi_M T$ of 3.5 $cm^3 K mol^{-1}$, indicating complete conversion to the metastable HS state (Figure 6, top). The light was then turned off and the sample warmed in the dark, according to our standardized *T*(LIESST) procedure described in the Experimental Section. The material remains in its HS state until 86 K, at which there is sudden fall in the $\chi_M T$ value to close to 0 $cm^3 K mol^{-1}$ equivalent to a complete relaxation to the LS ground state. The initial increase of the signal between 20–40 K is due to the zero-field splitting of the HS state, and the discontinuity in the plateau near 40 K is due to residual oxygen.

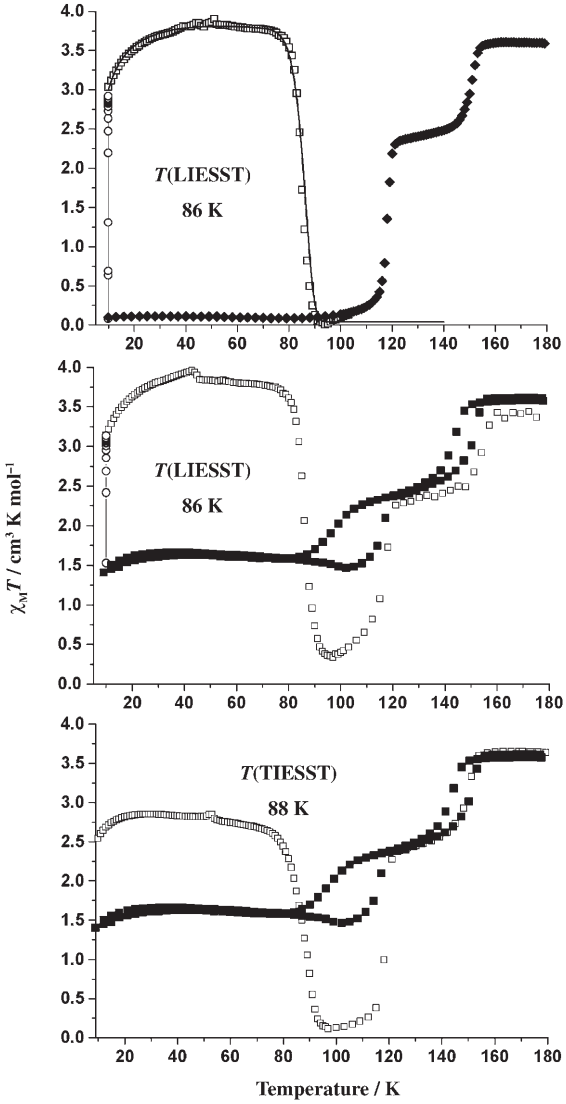

Figure 6. Excited high-spin state trapping and decay in $[FeL_2][BF_4]_2 \cdot x H_2O$. Top: generation and thermal decay of the metastable LIESST excited state, produced by laser irradiation of the fully low-spin state of the material. The curve presented in the LIESST region corresponds to the simulation obtained with the experimental kinetics parameters deduced from the study of the relaxations. Middle: generation and thermal decay of the metastable LIESST excited state, produced by laser irradiation of the mixed-spin phase of the material. Bottom: generation and thermal decay of the metastable excited state, produced by rapid thermal quenching of the high-spin state of the material. The data are in open circles, while the thermal magnetic behavior of the unirradiated starting material is shown in black circles for comparison.

We also performed light irradiation on the same sample, but cooled directly to 10 K at 1 K min^{-1} without annealing at 100 K. The material then possesses a residual HS fraction of approximately 46% at 10 K, as before (Figure 6, middle). The behavior of this spin-state population upon laser irradiation at 10 K and re-warming was identical to that observed for the fully LS form of the material. Most importantly, the compound relaxes to its fully LS form at 86 K, not to the approximately 46:54 HS:LS distribution found in the starting

material for the experiment. These results indicate that the same metastable HS state is reached following irradiation no matter what the LS population of the sample beforehand.

Finally, the metastable HS state of a spin-transition material can also often be generated by rapid thermal quenching of the sample (so-called thermally induced excited spin-state trapping, or TIESST).[43] Cooling the sample of $[FeL_2][BF_4]_2 \cdot x H_2O$ from room temperature to 10 K over a period of seconds afforded a residual $\chi_M T$ value of 2.5 $cm^3 K mol^{-1}$, indicating that approximately 70% of the compound had now been trapped in its HS form (Figure 6, bottom). When the temperature was increased following the same procedure used for the photomagnetic experiments, the data observed were very close to those obtained after light irradiation. Once more, this suggests that the metastable HS state afforded by thermal quenching exhibits a very similar structure to that reached by light irradiation.

Relaxation kinetics of metastable high-spin $[FeL_2][BF_4]_2 \cdot x H_2O$: Figure 7 displays the time dependence of the HS fraction of the sample, γ_{HS}, at selected temperatures between 10 K and the highest temperatures accessible with our SQUID magnetometer, which are close to T(LIESST). Analysis of these relaxations was performed by using a sigmoidal law, consistent with the self-accelerated behavior predicted for strongly cooperative systems. This deviation from a single exponential is, in fact, connected to the cooperativity arising from the large difference in metal–ligand bond lengths between the HS and LS states, and the resultant inelastic interactions caused by the change in internal pressure inside the solids as the spin transition proceeds.[44] The height of the activation barrier is, consequently, a function of γ_{HS}. The relaxation rate k_{HL}* depends exponentially on both γ_{HS} and T [Eqs. (2) and (3)], in which $\alpha(T)$ ($=E_a$*/$k_B T$) is the acceleration factor at a given temperature.

$$\frac{\partial \gamma_{HS}}{\partial T} = -k_{HL}{}^{*} \gamma_{HS} \quad (2)$$

$$k_{HL}{}^{*}(T,\gamma_{HS}) = k_{HL}(T)\exp[\alpha(T)(1-\gamma_{HS})] \quad (3)$$

Based on this treatment, the calculated curves of the relaxation are shown as solid lines in Figure 7. The apparent activation energy, $E_a = 1560\ cm^{-1}$, and the apparent pre-exponential factor, $k_8 = 4.5 \times 10^8\ s^{-1}$, of the activated region are calculated from the straight line given by plotting $\ln[k_{HL}(T)]$ versus $1/T$. The energy associated with the cooperativity E_a* is 25 cm^{-1}.

An elegant way to test the validity of these kinetic parameters is to use them to reproduce the experimental T(LIESST) curve.[15b,45] For this it is necessary to take into account carefully the time and temperature dependencies. The main difficulty of this simulation is to estimate satisfactorily the rate constant k_0 [that is, $k_{HL}(T \rightarrow 0)$], for relaxation by the quantum mechanical tunneling region. For this, we consider that the last complete kinetic measurement recorded at low temperature (that is, at 75 K, see Figure 7) can be regarded as an upper limit for the k_0 value ($=4.6 \times 10^{-5}\ s^{-1}$). The calculated T(LIESST) curve is plotted in Figure 6 (top) for the sample initially before irradiation prepared the LS form. The agreement with the experimental T(LIESST) curve is excellent, proving the validity of the derived kinetic parameters.

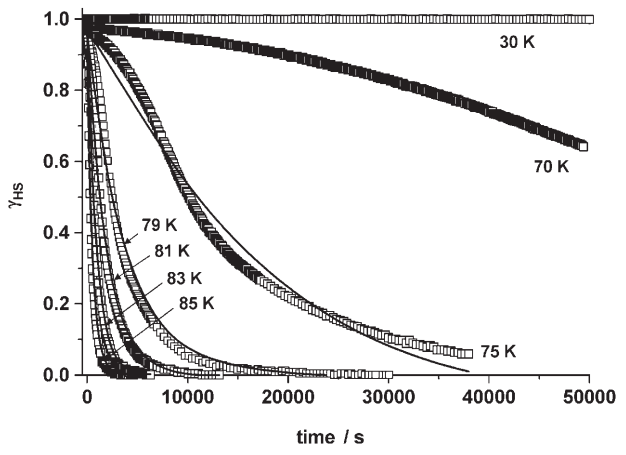

Figure 7. Time dependence at various temperatures of the HS molar fraction generated by laser irradiation of $[FeL_2][BF_4]_2 \cdot x H_2O$ at 10 K. Each point represents the high spin fraction deduced from the magnetic response measured within the SQUID magnetometer during around 30 s. The relaxation curves are fitted according to sigmoidal behavior (see text for more details).

Crystallographic characterization of $[FeL_2][BF_4]_2$: Initial crystallographic characterization was carried out by using an anhydrous crystal of formula $[FeL_2][BF_4]_2$. This crystallizes in the monoclinic space group $C2/c$ with unit cell parameters of $a = 23.341(5)$, $b = 11.000(2)$, $c = 24.037(5)$ Å, $\beta = 95.44(3)°$ and $V = 6144(2)$ $Å^3$ at 200 K. The asymmetric unit consists of one cation and two anions, and there are eight formula units in the unit cell. The iron atom occupies a distorted octahedral environment with two ligands bound equatorially through three of their five nitrogen atoms (Figure 8). The iron–nitrogen bond lengths were indicative of an HS iron(II) species (Table 4). On cooling to 130 K the crystal undergoes a crystallographic phase transition; the bulk packing remains the same with the space group still being $C2/c$ but the unit cell volume triples. The unit cell parameters are now: $a = 54.88(1)$, $b = 10.892(2)$, $c = 31.997(3)$ Å, $\beta = 109.77(3)°$ and $V = 17999(6)$ $Å^3$; there are three independent cations in the asymmetric unit and twenty four formula units in the unit cell. Close investigation of the metal–ligand bond lengths reveals that one of the independent cations is in the LS state (Fe1), whilst two are HS (Fe2 and Fe3; Table 4). Therefore, there are only very minor changes in the solid-state structure arising from this transition, which explains why the diffraction peaks for this larger cell appear as weak super cell peaks and thus give a comparatively poor quality of the structure solution. Whilst the mean metal–

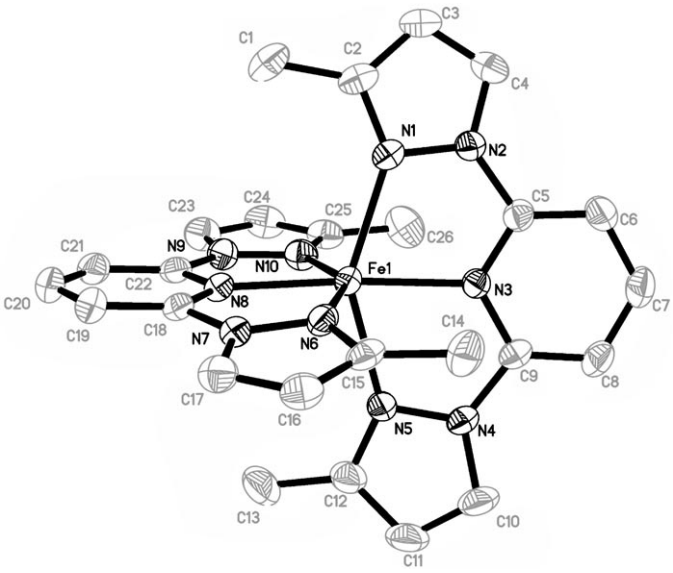

Figure 8. Structure of the $[FeL_2]^{2+}$ cation of $[FeL_2][BF_4]_2$ at 200 K. Hydrogen atoms have been omitted for clarity and thermal ellipsoids are at 50% probability.

Table 4. Selected molecular parameters for $[FeL_2][BF_4]_2$. See reference [46] for the definition of Σ.

T [K]	Fe	Spin state	Mean Fe–N [Å]	Bite angle [°]	Σ[°]
200	1	HS	2.166(3)	73.7(1)	153.1
130	1	LS	1.975(3)	80.1(1)	90.6
	2	HS	2.168(3)	73.5(1)	158.9
	3	HS/LS	2.130(3)	74.8(1)	143.7
90	1	LS	1.968(3)	80.08(1)	101.8

ligand bond length of Fe3 is in line with expectations for an HS iron(II) center, both it and the Σ parameter[46] are significantly lower than the values recorded for either Fe2 at 130 K or for the 100% HS structure at 200 K. This suggests that a small number of iron atoms at this site are in the LS state. The percentage in the LS state may be estimated by comparison with the Σ parameter for Fe2, which is assumed to be completely high spin, and that for Fe1, which is assumed to be completely low spin. This comparison indicates that approximately 20% of the Fe3 sites are in the LS state, and this is supported by significant differences in the structures of Fe2 and Fe3 and the elongation of the anisotropic temperature factors in Fe3 along the metal–ligand bonds and in the direction of the bite angle, which increases on going from the HS to the LS state. Examination of the intermolecular bonding and packing provides no conclusive reason as to why only a third of the molecules undergo a complete spin transition. Overall this analysis suggests that at 130 K around 40% of the molecules are in the LS state, which perfectly corroborates the magnetic data in Figure 1.

By cooling the crystal further to 90 K, we determined the structure of a fully LS state, in agreement with the magnetic data recorded after a kinetic relaxation at 100 K. The unit cell parameters are as follows: $a=22.707(5)$, $b=10.817(2)$, $c=24.162(5)$ Å, $\beta=93.11(3)°$, $V=5926(2)$ Å^3. The iron–nitrogen bond lengths are indicative of a completely low-spin iron centre and the Σ parameter shows that, as expected, the low-spin state is closer to the ideal octahedral geometry than the high-spin state (Table 4). Monitoring the evolution of the unit cell parameters with temperature upon cooling at the slow rate of $-3\,K\,h^{-1}$ shows that the HS state in the smaller unit cell is stable between 300 K and 160 K, the mixed-spin state with a unit cell volume of ≈ 18000 Å^3 is stable between 150 and 120 K, at which temperature the smaller cell is reformed indicating a complete transition to the LS state.

Unfortunately, crystals of anhydrous $[FeL_2][BF_4]_2$ collapse on further cooling to 30 K, so no examination of the excited state behavior of these crystals on irradiation or quenching was possible.

Crystallographic characterization of $[FeL_2][BF_4]_2\cdot{}^1/_3\,H_2O$: In the course of our X-ray diffraction studies we noticed that when a crystal is freshly prepared it contains a disordered water molecule, the formula of the crystal being $[FeL_2][BF_4]_2\cdot{}^1/_3\,H_2O$. The spin transition behavior of this compound is found to be significantly different to that observed for the dehydrated compound. Over a period of several weeks the crystals were observed to lose their water content without substantial loss of crystallinity.

Interestingly, the $[FeL_2][BF_4]_2\cdot{}^1/_3\,H_2O$ sample was found to be isostructural with the dehydrated compound at 200 K, crystallizing in the monoclinic space group $C2/c$ with unit cell parameters of $a=23.425(5)$, $b=11.000(2)$, $c=24.017(5)$ Å, $\beta=95.56(3)°$ and $V=6159(2)$ Å^3, but to contain a third of a disordered water molecule. The iron–nitrogen bond distances and symmetry parameter Σ (Table 5)[46] indicate that the compound is in the HS state at this temperature. The disordered water molecule is sited in a cavity of 30 Å^3, essentially equal to the volume of a water molecule (29.7 Å^3 in bulk water[47]), and the water oxygen atom forms a hydrogen bond with the methyl group of one of the ligands. Aside from the presence of the water molecule in the lattice, the packing of the hydrated compound remains the same as that of the dehydrated material. There are no significant differences between the structures of the HS cations at 200 K of the hydrated and dehydrated compounds. The loss of water from the crystal does not appear to affect the packing, intermolecular bonding or geometry of the compound. On cooling to 130 K $[FeL_2][BF_4]_2\cdot{}^1/_3\,H_2O$ is found to remain in the HS state with no significant differences between the

Table 5. Selected molecular parameters for $[FeL_2][BF_4]_2\cdot{}^1/_3H_2O$. See reference [46] for the definition of Σ.

T [K]	Fe	Spin state	Mean Fe–N [Å]	Bite angle [°]	Σ [°]
200	1	HS	2.165(2)	73.68(9)	155.9
130	1	HS	2.159(3)	73.8(1)	154.8
90	1	LS	1.985(9)	79.9(4)	95.8
	2	HS	2.168(9)	73.7(3)	156.0
	3	HS	2.15(1)	73.7(4)	158.2

structure determined at 200 K and that determined at 130 K. This behavior is in contrast to that observed for the hydrated compound, which at 130 K was found to exist in the mixed-spin state with a unit cell volume of $\approx$18000 Å^3. At 90 K $[FeL_2][BF_4]_2 \cdot {}^1/_3\,H_2O$ is found to be in the mixed-spin state with unit cell parameters of $a=55.28(1)$, $b=10.957(2)$, $c=31.973(6)$ Å, $\beta=108.88(3)°$ and $V=18325(6)$ Å^3 and to be in the monoclinic space group $C2/c$. The asymmetric unit consists of three formula units. Interestingly in this hydrated compound not only do the spin states order, giving one LS and two HS cations in the asymmetric unit, but the water molecules are also ordered, there now being two water molecules in the asymmetric unit with occupancies of one half. Although this is an extremely interesting aspect of the spin-crossover behavior of $[FeL_2][BF_4]_2 \cdot {}^1/_3\,H_2O$ it is unlikely to be the reason behind the formation of the mixed-spin state, as this behavior is observed in the dehydrated compound as well. It is perhaps self evident that the water molecules cannot play a very critical role in the intermolecular interactions of the crystal, as it is possible for a sample to lose water and still retain its crystallinity. Examination of the symmetry parameters and metal–ligand bond lengths for the three independent cations reveals that in the hydrated compound the cation containing Fe3 is fully high spin, as is that containing Fe2. Comparison of the structures of the cations from the mixed-spin state of the hydrated compound at 90 K with that of the dehydrated compound at 130 K reveals that there is no significant difference in the structure of the cations between the two compounds.

Numerous attempts were made to obtain a fully LS state by rapidly freezing the sample to 100 K and then allowing it to relax at this temperature, as reported in the $[FeL_2][BF_4]_2$ case, but in every case the mixed-spin state was found. The difficulty in reaching the fully lo-spin state for the hydrated compound in comparison to the dehydrated material, which is fully low-spin at this temperature, suggests that the presence of water acts to stabilize the HS state. However, we were successful in obtaining the structure of the metastable HS states of $[FeL_2][BF_4]_2 \cdot {}^1/_3\,H_2O$ resulting from both excitation with laser light and by flash freezing.

The structure of the mixed-spin state formed by cooling at 120 K h^{-1} from 300 to 30 K was close to that recorded 90 K, unit cell parameters: $a=54.91(1)$, $b=10.872(2)$, $c=31.710(6)$ Å, $\beta=108.94(3)°$ and $V=17905(6)$ Å^3. Irradiation of this mixed-spin state at 30 K with red laser light ($\lambda=632.8$ nm, 25 mW) for ten minutes promoted the crystal to the metastable HS state. The unit cell parameters after irradiation are: $a=23.078(5)$, $b=10.948(2)$, $c=23.797(5)$ Å, $\beta=95.66(3)°$ and $V=5983(2)$ Å^3. The symmetry parameters and iron–nitrogen bond lengths show that the compound is in the HS state, with only one independent cation. On warming from 30 K the crystal remains in the metastable HS state until 90 K, whereupon it undergoes relaxation back into the mixed-spin state.

Another route by which the metastable HS state may be reached is by rapid cooling of the crystal to very low temperature.[43] Flash freezing of the crystal in a flow of chilled helium gas at 30 K gave rise to an HS state with unit cell parameters of $a=23.229(5)$, $b=0.935(2)$, $c=23.801(5)$ Å, $\beta=96.02(3)°$ and $V=6012(2)$ Å^3. Comparison of the structure of the flash-frozen crystal with that of the irradiated crystal shows that there are no significant differences between the two HS states. The structure of the LS state of $[FeL_2][BF_4]_2 \cdot {}^1/_3 H_2O$ was finally determined by warming the flash-frozen crystal at 120 K h^{-1} from 30 to 90 K and allowing it to relax at this temperature for one hour. If the temperature is allowed to rise above this the mixed-spin state is reformed. The crystal was then cooled from 90 to 30 K, and a full crystallographic structure determination was undertaken. Visual examination of the diffraction data shows that there is some evidence of diffracted X-ray intensity between the sharp diffraction peaks, suggesting that under these conditions some of the crystal is still in the mixed-spin state; this observation is supported by the pronounced degree of distortion observable both along the metal–ligand bonds and, for the pyrazole nitrogen atoms in particular, in the direction of the ligand bite angle on refinement.

Discussion

Our combined susceptibility and crystallographic measurements have demonstrated that spin-crossover in $[FeL_2][BF_4]_2 \cdot x\,H_2O$ is kinetically slow, with the compound becoming trapped in a metastable mixed-spin state when cooled from room temperature at "normal" rates. High kinetic barriers to spin-crossover have been demonstrated before in a small number of iron(II) compounds, with $T_{1/2} < 100$ K. This typically leads to thermal quenching of a fraction of the sample in its HS state upon cooling, so that the fully LS material cannot be accessed by cooling from room temperature.[48] However, the existence of an intermediate LS phase has only been demonstrated in two other spin transition systems, namely $[Fe(pic)_3]Cl_2 \cdot H_2O$ (pic = 2-{aminomethyl}pyridine)[49] and $[Fe(ptz)_6][BF_4]_2$ (ptz = 1-*n*-propyltetrazole).[50] Rapid cooling of these compounds reveals a metastable, intermediate LS phase, which converts slowly to a second, thermodynamically stable LS phase upon annealing just below the thermal transition temperature. Slower cooling of both materials from room temperature affords the thermodynamic LS state directly. The HS and metastable ("ordered") LS phases of $[Fe(ptz)_6][BF_4]_2$ are isostructural,[51,52] while its stable ("disordered") LS phase is apparently amorphous.[51,53] No structural data for $[Fe(pic)_3]Cl_2 \cdot H_2O$ are available.

Importantly, however, these two literature compounds differ from $[FeL_2][BF_4]_2 \cdot x H_2O$ in two ways (Scheme 1). First, re-warming the thermodynamic LS phases of $[Fe(pic)_3]Cl_2 \cdot H_2O$ and $[Fe(ptz)_6][BF_4]_2$ affords their HS phases directly, without passing through their metastable intermediate phase. In contrast, the thermal LS–HS transition in $[FeL_2][BF_4]_2 \cdot x\,H_2O$ does involve its mixed-spin intermediate phase, at least in the dehydrated material (see below).

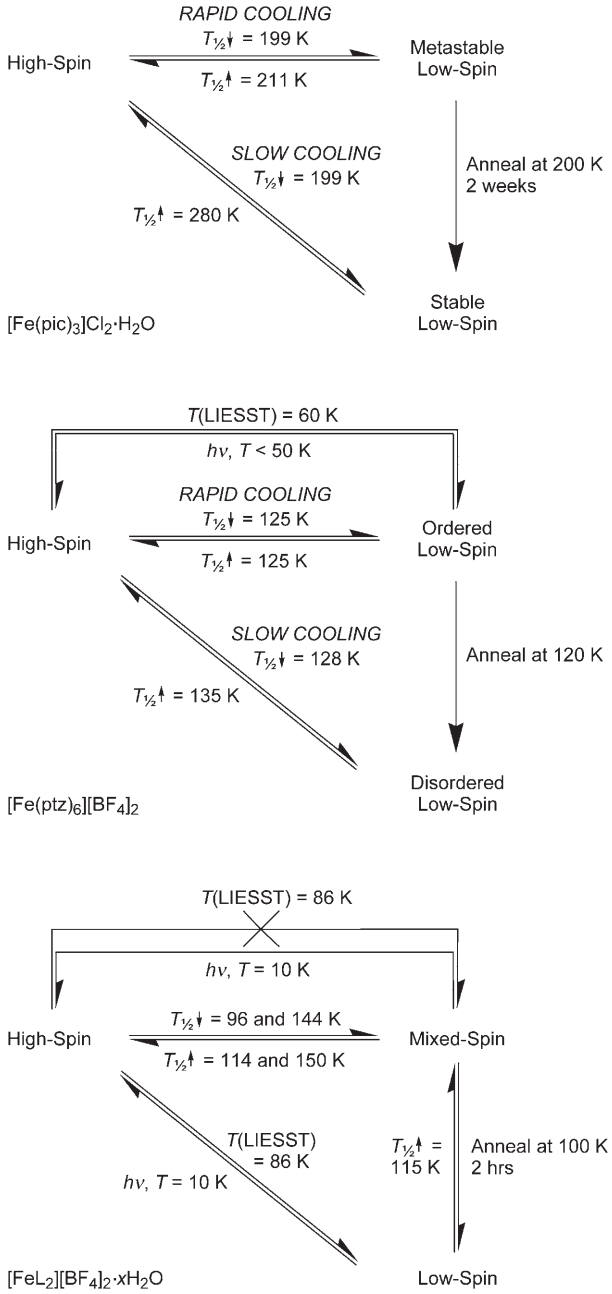

Scheme 1. Comparison of the thermal and photochemical spin-transition behavior of $[Fe(pic)_3]Cl_2 \cdot H_2O$,[49] $[Fe(ptz)_6][BF_4]_2$,[50] and $[FeL_2][BF_4]_2 \cdot xH_2O$, involving metastable spin-transition intermediates.

Second, relaxation of the LIESST HS state of $[Fe(ptz)_6][BF_4]_2$, which takes place at 50 K, affords the metastable ("ordered") LS phase of this material only.[54] This is to be expected, since T(LIESST) for this material (50 K) lies substantially below the kinetic barrier for the "ordered"→"disordered" LS phase transition. However, the fully LS, thermodynamic phase of $[FeL_2][BF_4]_2 \cdot x H_2O$, is generated *directly* upon thermal relaxation of the metastable, thermally or photochemically trapped HS form, without passing through the mixed-spin phase. This is emphasized by the kinetics of the relaxation process, which are well reproduced by a simple sigmoidal model without any requirement for an intermediate species.

The apparent role of lattice water in $[FeL_2][BF_4]_2 \cdot x H_2O$ is also remarkable. We attribute the two-step nature of the thermal HS to mixed-spin interconversion in the bulk material to the existence of different regions of hydrated and dehydrated material in the bulk solid; these regions undergo spin-crossover at 105 and 147 K respectively, with hysteresis. As the compound is aged, the remaining water is lost and the plateau in the transition disappears. The effect is also observed in a single crystal of the material, in that the same crystal undergoes the HS to mixed-spin phase transition at 110 ± 20 K when hydrated, and at 155 ± 5 K when aged and dehydrated. It is worth noting, however, that relaxation of the LIESST excited state of the whole powder sample directly from its HS to its LS state takes place at a single temperature. This shows that LIESST relaxation in $[FeL_2][BF_4]_2 \cdot x H_2O$ is independent of x (compare with references [20] and [55] for example, in which heterogeneous iron environments in LIESST samples were reflected in a distribution of relaxation temperatures upon warming).

The observations in the two previous paragraphs all strongly imply that the thermal HS⇔LS interconversion at 94 K and above, and the thermally activated HS⇔LS LIESST relaxation at 86 K, occur through different mechanistic pathways. The former proceeds through the mixed-spin intermediate phase and depends on x, while the latter avoids the mixed-spin phase and is independent of x. Such a change in mechanism can only occur as a result of structural and energetic differences between the thermally stable and quenched metastable HS states of the material. Although we have no structural data for the HS state at 30 K when $x = 0$, when $x = {}^1/_3$ the HS states at 200 and 30 K are isostructural and display no detectable structural differences at the molecular level (see Supporting Information). Therefore, the different pathways of HS to LS conversion are likely to be a consequence of more subtle changes in crystal pressure, caused by anisotropic contraction of the crystals upon cooling. It is well established that such changes in crystal pressure can lead to detectable differences in the molecular structures of thermally stable and photogenerated metastable HS states of iron(II) complexes.[56] Although not observed for $[FeL_2][BF_4]_2 \cdot x H_2O$, this is the first example of a spin-crossover compound in which these effects apparently cause a more fundamental change in the functional cooperativity of the material at different temperatures.

While the transition temperatures from our magnetochemical and crystallographic analyses are in good agreement, there is a discrepancy in the composition of the mixed-spin phase between the two techniques. The $\chi_M T$ value of 1.6 $cm^3 K mol^{-1}$ consistently shown by the mixed-spin phase implies that it contains an approximate 46:54 ratio of HS and LS material. However, the crystallographic experiments imply that the mixed-spin phase is 60–66 % HS, depending on x. We tentatively attribute these differences to the effects of grinding the crystalline sample to a powder for the SQUID measurements, since SCO in several molecular

compounds (including one related to this one[57]) has been shown to depend markedly on sample preparation.[57,58] One alternative explanation, that the bulk material contains a contaminant phase that is fully LS below 130 K,[21] is ruled out by the powder diffraction and photomagnetic data.

To conclude, we have successfully prepared and investigated the magnetic and photomagnetic properties of the first spin-transition material, the long-lived metastable HS excited state of which was predicted to relax at a higher temperature than its thermal SCO (Figure 1). We have shown that the thermal SCO is strongly dependent on kinetic phenomena in this situation, and that thermal HS to LS conversion and thermally activated HS to LS relaxation in this material proceed by different kinetic pathways. This results in a reduction in T(LIESST) from the value predicted by Equation (1), thus avoiding the physical impossibility of T(LIESST) being greater than $T_{1/2}$. These results emphasize that full characterization of both thermal and photomagnetic properties is necessary in the continued quest to maximize T(LIESST) in materials for new photoswitchable devices.

Acknowledgements

The authors acknowledge the EPSRC for two studentships, (V.A.M. and J.E.) and for a Senior Research Fellowship (J.A.K.H.), the British Council/CNRS Alliance initiative (M.A.H., J.-F.L.) and the Aquitain region for funding. David Wright (Institute of Materials Research, University of Leeds) is thanked for the powder diffraction measurements, while Dr. Harry Blythe (University of Sheffield) and Dr. Mike Jeggo (University of Cambridge) are acknowledged for the magnetochemical data in the Supporting Information.

[1] For general reviews, see: *Topics in Current Chemistry Vol. 233–235: Spin-Crossover in Transition-Metal Compounds* (Eds.: P. Gutlich, H. A. Goodwin), Springer, Berlin, **2004**.
[2] a) O. Kahn, J. Kröber, C. J. Martinez, *Adv. Mater.* **1992**, *4*, 718; b) J.-F. Létard, P. Guionneau, E. Codjovi, O. Lavastre, G. Bravic, D. Chasseau, O. Kahn, *J. Am. Chem. Soc.* **1997**, *119*, 10861.
[3] a) E. Freysz, S. Montant, S. Létard, J.-F. Létard, *Chem. Phys. Lett.* **2004**, *394*, 318; b) S. Bonhommeau, G. Molnár, A. Galet, A. Zwick, J. A. Real, J. J. McGarvey, A. Bousseksou, *Angew. Chem.* **2005**, *117*, 4137; *Angew. Chem. Int. Ed.* **2005**, *44*, 4069.
[4] S. Decurtins, P. Gütlich, C. P. Köhler, H. Spiering, A. Hauser, *Chem. Phys. Lett.* **1984**, *105*, 1.
[5] E. König, *Prog. Inorg. Chem.* **1987**, *35*, 527.
[6] A. Hauser in *Topics in Current Chemistry, Vol. 234,* (Eds.: P. Gutlich, H. A. Goodwin), Springer, Berlin, **2004**, p. 155.
[7] a) T. Buchen, P. Gütlich, H. A. Goodwin, *Inorg. Chem.* **1994**, *33*, 4573; b) T. Buchen, P. Gütlich, K. H. Sugiyarto, H. A. Goodwin, *Chem. Eur. J.* **1996**, *2*, 1134; c) C. H. Wu, J. Jung, P. K. Gantzel, P. Gütlich, D. N. Hendrickson, *Inorg. Chem.* **1997**, *36*, 5339; d) F. Renz, H. Oshio, V. Ksenofontov, M. Waldeck, H. Spiering, P. Gütlich, *Angew. Chem.* **2000**, *112*, 3832; *Angew. Chem. Int. Ed.* **2000**, *39*, 3699; e) S. Hayami, Z.-Z. Gu, Y. Einaga, Y. Kobayashi, Y. Ishikawa, Y. Yamada, A. Fujishima, O. Sato, *Inorg. Chem.* **2001**, *40*, 3240.
[8] a) O. Kahn, C. J. Martinez, *Science* **1998**, *279*, 44; b) O. Kahn, C. J. Martinez, J. Kröber, R. Claude, F. Grolière, Patent, **1995** EP0666561; c) J.-F. Létard, O. Nguyen, N. Daro, Patent, **2005** FR0512476.
[9] J.-F. Létard, P. Guionneau, L. Goux-Capes, in *Topics in Current Chemistry, Vol. 235* (Eds.: P. Gutlich, H. A. Goodwin), Springer, Berlin, **2004**, p. 221.
[10] a) A. Bousseksou, G. Molnár, P. Demont, J. Menegotto, *J. Mater. Chem.* **2003**, *13*, 2069; b) S. Bonhommeau, T. Guillon, L. M. L. Daku, P. Demont, J. S. Costa, J.-F. Létard, G. Molnár, A. Bousseksou, *Angew. Chem.* **2006**, *118*, 1655; *Angew. Chem. Int. Ed.* **2006**, *45*, 1625.
[11] A. Bousseksou, C. Vieu, J.-F. Létard, P. Demont, J.-P. Tuchagues, L. Malaquin, J. Menegotto, L. Salmon, EP1430552, **2004**.
[12] R. N. Muller, L. van der Elst, S. Laurent, *J. Am. Chem. Soc.* **2003**, *125*, 8405.
[13] a) W. R. Scheidt, C. A. Reed, *Chem. Rev.* **1981**, *81*, 543; b) M. F. Perutz, G. Fermi, B. Luisi, B. Shannan, R. C. Liddington, *Acc. Chem. Res.* **1987**, *20*, 309; c) D. R. Davydov, G. H. B. Hoa, J. A. Peterson, *Biochemistry* **1999**, *38*, 751; d) J. Badro, G. Fiquet, F. Guyot, J. P. Rueff, V. V. Struzhin, G. Vanko, G. Monaco, *Science* **2003**, *300*, 789.
[14] J.-F. Létard, P. Guionneau, L. Rabardel, J. A. K. Howard, A. E. Goeta, D. Chasseau, O. Kahn, *Inorg. Chem.* **1998**, *37*, 4432.
[15] a) J.-F. Létard, P. Guionneau, O. Nguyen, J. S. Costa, S. Marcén, G. Chastanet, M. Marchivie, L. Capes, *Chem. Eur. J.* **2005**, *11*, 4582; b) J.-F. Létard, *J. Mater. Chem.* **2006**, *16*, 2550.
[16] J.-F. Létard, J. S. Costa, S. Marcen, C. Carbonera, C. Desplanches, A. Kobayashi, N. Daro, P. Guionneau, *J. Phys. Conf. Ser.* **2005**, *21*, 23.
[17] J.-F. Létard, L. Capes, G. Chastanet, N. Moliner, S. Létard, J. A. Real, O. Kahn, *Chem. Phys. Lett.* **1999**, *313*, 115.
[18] S. Marcén, L. Lecren, L. Capes, H. A. Goodwin, J.-F. Létard, *Chem. Phys. Lett.* **2002**, *358*, 87.
[19] V. A. Money, J. S. Costa, S. Marcén, G. Chastanet, J. Elhaúk, M. A. Halcrow, J. A. K. Howard, J.-F. Létard, *Chem. Phys. Lett.* **2004**, *391*, 273.
[20] C. Carbonera, J. S. Costa, V. A. Money, J. Elhaúk, J. A. K. Howard, M. A. Halcrow, J.-F. Létard, *Dalton Trans.* **2006**, 3058.
[21] N. Shimamoto, S.-S. Ohkoshi, O. Sato, K. Hashimoto, *Inorg. Chem.* **2002**, *41*, 678.
[22] A. Hauser, *Coord. Chem. Rev.* **1991**, *111*, 275.
[23] M. A. Halcrow, *Coord. Chem. Rev.* **2005**, *249*, 2880.
[24] J. M. Holland, J. A. McAllister, Z. Lu, C. A. Kilner, M. Thornton-Pett, M. A. Halcrow, *Chem. Commun.* **2001**, 577.
[25] J. M. Holland, J. A. McAllister, C. A. Kilner, M. Thornton-Pett, A. J. Bridgeman, M. A. Halcrow, *J. Chem. Soc. Dalton Trans.* **2002**, 548.
[26] V. A. Money, I. R. Evans, M. A. Halcrow, A. E. Goeta, J. A. K. Howard, *Chem. Commun.* **2003**, 158.
[27] J. Elhaúk, V. A. Money, S. A. Barrett, C. A. Kilner, I. R. Evans, M. A. Halcrow, *Dalton Trans.* **2003**, 2053.
[28] V. A. Money, I. R. Evans, J. Elhaúk, M. A. Halcrow, J. A. K. Howard, *Acta Crystallogr. Sect. B* **2004**, *60*, 41.
[29] V. A. Money, J. Elhaúk, M. A. Halcrow, J. A. K. Howard, *Dalton Trans.* **2004**, 65.
[30] V. A. Money, J. Elhaúk, M. A. Halcrow, J. A. K. Howard, *Dalton Trans.* **2004**, 1516.
[31] J. M. Holland, S. A. Barrett, C. A. Kilner, M. A. Halcrow, *Inorg. Chem. Commun.* **2002**, *5*, 328.
[32] J. Elhaïk, C. A. Kilner, M. A. Halcrow, *Dalton Trans.* **2006**, 823.
[33] a) H. A. Goodwin, R. N. Sylva, *Aust. J. Chem.* **1968**, *21*, 83; b) A. T. Baker, H. A. Goodwin, *Aust. J. Chem.* **1986**, *39*, 209; c) D. Onggo, J. M. Hook, A. D. Rae, H. A. Goodwin, *Inorg. Chim. Acta* **1990**, *173*, 19; d) A. T. Baker, P. Singh, V. Vignevich, *Aust. J. Chem.* **1991**, *44*, 1041; e) E. C. Constable, G. Baum, E. Bill, R. Dyson, R. van Eldik, D. Fenske, S. Kaderli, D. Morris, A. Neubrand, M. Neuburger, D. R. Smith, K. Wieghardt, M. Zehnder, A. D. Zuberbühler, *Chem. Eur. J.* **1999**, *5*, 498.
[34] SMART-1000 CCD, Bruker AXS, Madison, Wisconsin, U.S.A
[35] Cryostream Cooler, Oxford Cryosystems Ltd, Oxford (UK).
[36] Oxford Helix, Oxford Cryosystems Ltd, Oxford (UK).
[37] A. E. Goeta, L. K. Thompson, C. L. Sheppard, S. S. Tandon, C. W. Lehmann, J. Cosier, C. Webster, J. A. K. Howard, *Acta Crystallogr. Sect. C* **1999**, *55*, 1243.
[38] SAINTPLUS v. 6.02. Data reduction software, Bruker AXS, Madison, WI (USA).

[39] G. M. Sheldrick, SHELXTL v. 5.1. An integrated system for solving, refining and displaying crystal structures from diffraction, Bruker AXS, Madison, WI (USA), **1999**.
[40] C. O'Connor, *J. Prog. Inorg. Chem.* **1982**, *29*, 203.
[41] K. Nakamoto, *Infrared and Raman Spectra of Inorganic and Coordination Compounds, Part B*, 5th ed., Wiley Interscience, New York, **1997**, p. 54.
[42] A. Desaix, O. Roubeau, J. Jeftic, J. G. Haasnoot, K. Boukheddaden, E. Codjovi, J. Linares, M. Nogues, F. Varret, *Eur. Phys. J. B* **1998**, *6*, 183.
[43] M. Marchivie, P. Guionneau, J.-F. Létard, D. Chasseau, J. A. K. Howard, *J. Phys. Chem. Solids* **2004**, *65*, 17 and refs. therein.
[44] A. Hauser, *Chem. Phys. Lett.* **1992**, *192*, 65.
[45] J.-F. Létard, G. Chastanet, O. Nguyen, S. Marcen, M. Marchivie, P. Guionneau, D. Chasseau, P. Gütlich, *Monatsh. Chem.* **2003**, *134*, 165.
[46] P. Guionneau, C. Brigouleix, Y. Barans, A. E. Goeta, J.-F. Létard, J. A. K. Howard, J. Gaultier, D. Chasseau, *C. R. Acad. Sci. Ser. IIc Chim.* **2001**, *4*, 161.
[47] M. Gerstein, J. Tsai, M. Levitt, *J. Mol. Biol.* **1995**, *249*, 955.
[48] a) G. Ritter, E. König, W. Irler, H. A. Goodwin, *Inorg. Chem.* **1978**, *17*, 224; b) R. Hinek, H. Spiering, P. Gütlich, A. Hauser, *Chem. Eur. J.* **1996**, *2*, 1435; c) N. Moliner, A. B. Gaspar, M. C. Muñoz, V. Niel, J. Cano, J. A. Real, *Inorg. Chem.* **2001**, *40*, 3986; d) A. B. Gaspar, M. C. Muñoz, N. Moliner, V. Ksenofontov, G. Levchenko, P. Gütlich, J. A. Real, *Monatsh. Chem.* **2003**, *134*, 285.
[49] a) M. Sorai, J. Ensling, K. M. Hasselbach, P. Gütlich, *Chem. Phys.* **1977**, *20*, 197; b) T. Nakamoto, A. Bhattacharjee, M. Sorai, *Bull. Chem. Soc. Jpn.* **2004**, *77*, 921.
[50] J. Kusz, P. Gütlich, H. Spiering, in *Topics in Current Chemistry, Vol. 234* (Eds.: P. Gutlich, H. A. Goodwin), Springer, Berlin, **2004**, p. 129 and references therein.
[51] L. Wiehl, *Acta Crystallogr. Sect. B* **1993**, *49*, 289.
[52] Y. Moritomo, K. Kato, A. Nakamoto, N. Kojima, E. Nishibori, M. Takata, M. Sakata, *J. Phys. Soc. Jpn.* **2002**, *71*, 1015.
[53] L. Wiehl, H. Spiering, P. Gütlich, K. Knorr, *J. Appl. Crystallogr.* **1990**, *23*, 151.
[54] N. O. Moussa, G. Molnár, X. Ducros, A. Zwick, T. Tayagaki, K. Tanaka, A. Bousseksou, *Chem. Phys. Lett.* **2005**, *402*, 503.
[55] See for example, G. S. Matouzenko, J.-F. Létard, S. Lecoeq, A. Bousseksou, L. Capes, L. Salmon, M. Perrin, O. Kahn, A. Collet, *Eur. J. Inorg. Chem.* **2001**, 2935.
[56] a) J. Kusz, H. Spiering, P. Gütlich, *J. Appl. Crystallogr.* **2001**, *34*, 229; b) M. Marchivie, P. Guionneau, J. A. K. Howard, G. Chastanet, J.-F. Létard, A. E. Goeta, D. Chasseau, *J. Am. Chem. Soc.* **2002**, *124*, 194; c) E. J. MacLean, C. M. McGrath, C. J. O'Connor, C. Sangregorio, J. M. W. Seddon, E. Sinn, F. E. Sowrey, S. J. Teat, A. E. Terry, G. B. M. Vaughan, N. A. Young, *Chem. Eur. J.* **2003**, *9*, 5314; d) A. L. Thompson, A. E. Goeta, J. A. Real, A. Galet, M. C. Muñoz, *Chem. Commun.* **2004**, 1390; e) N. Huby, L. Guérin, E. Collet, L. Toupet, J.-C. Ameline, H. Cailleau, T. Roisnel, T. Tayakagi, K. Tanaka, *Phys. Rev. B* **2004**, *69*, 20101.
[57] J. Elhaïk, D. J. Evans, C. A. Kilner, M. A. Halcrow, *Dalton Trans.* **2005**, 1693.
[58] See *for example*, a) M. S. Haddad, W. D. Federer, M. W. Lynch, D. N. Hendrickson, *Inorg. Chem.* **1981**, *20*, 131; b) E. W. Müller, H. Spiering, P. Gütlich, *Chem. Phys. Lett.* **1982**, *93*, 567; c) E. W. Müller, H. Spiering, P. Gütlich, *J. Chem. Phys.* **1983**, *79*, 1439; d) E. W. Müller, H. Spiering, P. Gütlich, *Inorg. Chem.* **1984**, *23*, 119; e) W. D. Federer, D. N. Hendrickson, *Inorg. Chem.* **1984**, *23*, 3870; f) A. F. Stassen, E. Dova, J. Ensling, H. Schenk, P. Gütlich, J. G. Haasnoot, J. Reedijk, *Inorg. Chim. Acta* **2002**, *335*, 61; g) D. J. Rudd, C. R. Goldsmith, A. P. Cole, T. D. P. Stack, K. O. Hodgson, B. Hedman, *Inorg. Chem.* **2005**, *44*, 1221.

Received: September 11, 2006
Published online: March 8, 2007

